Biochimica et Biophysica Acta 892 (1987) 30–41
Elsevier

BBA 42542

Novel approaches towards characterization of the high-affinity nucleotide binding sites on mitochondrial F_1-ATPase by the fluorescence probes 3′-*O*-(1-naphthoyl)adenosine di- and triphosphate

Joachim Weber [a], Matthias Rögner [b] and Günter Schäfer [a]

[a] *Institut für Biochemie, Medizinische Universität zu Lübeck, Lübeck (F.R.G.) and* [b] *Max-Volmer-Institut für Biophysikalische und Physikalische Chemie, Technische Universität Berlin, Berlin (Germany)*

(Received 24 September 1986)

Key words: Fluorescence probe; Nucleotide analog; Nucleotide binding; ATPase, F_1-; High-affinity binding site

The fluorescence properties of 3′-*O*-(1-naphthoyl)adenosine di- and triphosphates (termed N-ADP and N-ATP, respectively) were investigated in detail. Of special importance for the use of these analogues as environmental probes is their high quantum yield (0.58 in water) and the polarity dependence of shape and wavelength position of the emission spectrum. Upon binding of N-ADP and N-ATP to mitochondrial F_1-ATPase, the fluorescence intensity is markedly decreased, due to polarity changes and 'ground-state' quenching. Using this signal for equilibrium binding studies, three (at least a priori) equivalent nucleotide-binding sites were detected on the enzyme. The perspective intrinsic dissociation constants are as follows: N-ADP/Mg^{2+} 120 nM; N-ATP/Mg^{2+} 160 nM; N-ADP/EDTA 560 nM; N-ATP/EDTA 3500 nM. For bound ligand the environment was found to be rather unpolar; the rotational mobility of the fluorophore is restricted, its accessibility for iodide anions (as a quencher) is hindered. These facts show a location of the binding sites quite deeply embedded in the protein. The conformation of the binding domains is strongly dependent on the absence or presence of Mg^{2+}, as can be seen from the relative efficiencies of the singlet-singlet energy transfer from tyrosine residues in the protein to bound naphthoyl moieties. Investigation of the binding kinetics revealed this process as biphasic (in presence of Mg^{2+}). After the first fast step ($k_{on} > 1 \cdot 10^6\ M^{-1} \cdot s^{-1}$), in which the analogue is bound to the enzyme, a slow local conformational rearrangement occurs.

Enzymes and abbreviations: F_1-ATPase, soluble part of the proton-translocating adenosine triphosphatase complex from bovine heart mitochondria (EC 3.6.1.34); pyruvate kinase (EC 2.7.1.40); lactate dehydrogenase (EC 1.1.1.27); *photinus* luciferin 4-monooxygenase (ATP-hydrolyzing) or luciferase (EC 1.13.12.7); N-AD(M,T)P, 3′-*O*-(1-naphthoyl)adenosine di(mono,tri)phosphate; *lin*-benzo-ADP, 8-amino-3-(β-D-ribofuranosyl)imidazo[4,5-*g*]quinazoline 5′-diphosphate.

Correspondence: J. Weber and G. Schäfer, Institut für Biochemie, Medizinische Universität zu Lübeck, Ratzeburger Allee 160, D-2400 Lübeck 1, F.R.G.

Introduction

The susceptibility of fluorescence to environmental changes makes fluorescence spectroscopy a sensitive tool for the investigation of ligand binding sites on proteins. Since most natural ligands are effectively non-fluorescent, covalent attachment of a fluorescent moiety to the respective ligand is a widely used approach. When comparability of the binding behaviour of the fluorescent

derivatives and the natural ligand has been proved, e.g., by competition experiments, this method offers several advantages. Besides equilibrium binding constants (number of binding sites and dissociation constants), additional information about the microenvironment at these sites can be obtained, regarding electronical (especially polarity) and specific structural properties.

For investigation of the adenine nucleotide binding sites on mitochondrial F_1-ATPase a wide variety of fluorescent nucleotide analogues has been analyzed [1–5] (for a recent review, see Ref. 6). In two previous studies [7,8] we communicated on the use of an ADP derivative for this purpose, at which the 3′-hydroxyl group of the ribose has been esterified with 1-naphthoic acid. This fluorescent analogue (3′-*O*-(1-naphthoyl)ADP, termed N-ADP) was found to bind to isolated [7] and membrane-bound [8] F_1-ATPase with high affinity.

In contrast to previous expectations, binding of N-ADP to the enzyme did not result in a fluorescence enhancement as frequently observed when a fluorophore enters a less polar environment. However, fluorescence anisotropy could be used as a parameter to monitor binding very sensitively due to (partial) immobilization of the naphthoyl residue. More recently, in studies on interaction of the respective triphosphate derivative, N-ATP, with F_1 from the thermophilic bacterium PS3, a significant influence on the shape of the emission spectrum of the ligand has been discovered [9]. One parameter describing these spectral changes has been tentatively used to determine thermodynamic binding constants. First attempts to repeat these experiments with bovine heart mitochondrial F_1 revealed that the fluorescence response of N-AD(T)P is complex and that a straightforward analysis encounters difficulties.

This prompted us to the present study focusing on two main aspects: (1) detailed reinvestigation of the fluorescence properties of N-ADP under various environmental conditions; and (2), on the basis of these informations, probing the environment of the fluorophore at the nucleotide-binding sites of mitochondrial F_1-ATPase.

It will be shown that, by careful selection of appropriate fluorescence parameters, 3′-*O*-(1-naphthoyl)adenosine phosphates are versatile environmental probes. Besides corroboration of the existence of three reversible high-affinity binding sites on F_1, this study adds further information about the topography of these sites, including mobility of bound ligand as well as nature and spatial relationship of specific neighbouring groups; in addition, N-AD(T)P enables a time-resolved analysis of the binding process.

Materials and Methods

Chemicals

1-Naphthoic acid was purchased from Aldrich (Steinheim). Boehringer (Mannheim) supplied AMP, ADP, ATP, NADH, phospho*enol*pyruvate, firefly luciferin, and the enzymes pyruvate kinase, lactate dehydrogenase, and firefly lucyferase. All other chemicals were of analytical or spectroscopical purity grade, obtained from Sigma (Deisenhofen) and Merck (Darmstadt).

Synthesis and characterization of 1-naphthoyl derivatives

Synthesis of 3′-*O*-(1-naphthoyl)adenosine di(mono,tri)phosphate has been described previously [10,11]; the product was characterized by NMR spectroscopy [11]. Concentrations of aqueous solutions of N-AD(M,T)P were measured by ultraviolet spectroscopy using absorption coefficients $\epsilon_{259\,nm} = 16\,000\ M^{-1} \cdot cm^{-1}$ and $\epsilon_{298\,nm} = 6\,400\ M^{-1} \cdot cm^{-1}$ (pH 8.0).

1-Naphthoic acid methyl ester was synthesized by standard methods for esterification, and characterized by melting point and refractive index [12].

Enzyme preparation and analysis

Nucleotide-depleted F_1-ATPase was prepared from bovine heart mitochondria as described in Ref. 13, with some minor modifications [7]. The remaining content of nucleotides was below 0.4 mol adenosine phosphates per mol enzyme, as determined by the luciferin/luciferase method [7]. The enzyme was stored in small aliquots at −80 °C in a buffer comprising 100 mM Tris-sulfate/5 mM EDTA/50% glycerol (pH 8.0). Each aliquot was used for only one set of experiments performed within 12 h of thawing; repetitive thawing and freezing leads to alterations especially of the binding kinetics.

Protein concentrations were determined by the method of Lowry et al. [14] using bovine serum albumin as a standard; the molecular mass of F_1 was taken to be 370 kDa [15]. ATPase activity (defined as μmol ATP hydrolyzed per min at 30 °C) was measured photometrically in an ATP-regenerating test system [16].

Fluorescence methods

All fluorescence measurements were carried out on a spectrofluorometer type SLM 4800 S. A general outline of the experimental approaches, including lifetime and polarization measurements, is given in Ref. 7.

For measuring quantum yields (Φ_F), the emission spectra were corrected for wavelength-dependence of the photomultiplier response [17]. The quantum yield was calculated from the area of the respective corrected spectrum on a wavenumber scale, using quinine sulfate (in 0.05 M H_2SO_4) as a standard, whose Φ_F was taken to be 0.70 [18]. Other results are derived from not-corrected emission spectra. However, it should be noted that the correction factors are close to unity in the wavelength range of interest; for comparison, see the emission spectra of N-ADP given in Fig. 1 (corrected) and Fig. 2 (uncorrected).

The average wavenumber of the emission spectrum was obtained graphically at half height of the net emission maximum. Excitation polarization spectra are based on continuously recorded spectra using an instrumental arrangement as described in Ref. 19, with subsequent computation of the resulting anisotropies in intervals of 2.5 or 5 nm.

For N-AD(T)P bound to F_1, depolarization due to some rotational motion of the enzyme within the lifetime of the excited state of the fluorophore was estimated by the Perrin equation. The rotational correlation time of F_1 was taken to be 190 ns; this value is based on the given molecular mass and the assumption of the protein being shaped as an oblate with an axial ratio of 2 : 1, which is a reasonable approximation for the actual shape [20]. The data presented for the cone half-angle describing the residual rotational mobility of bound fluorophore were calculated according to Ref. 21.

Relative efficiencies, E_r, of the Förster-type energy-transfer are given as enhancement of acceptor fluorescence due to the transfer. Data were calculated from the ratio, H, of fluorescence intensities of the acceptor in presence and absence of donor (λ_{exc} 279 nm, λ_{em} 395 nm), normalized by the ratio at an excitation wavelength of 320 nm (λ_{em} 395 nm) at which no energy transfer is measurable, to correct for static quenching observed upon binding:

$$E_r = \frac{H_{\text{exc 279 nm}}}{H_{\text{exc 320 nm}}} - 1 \qquad (1)$$

Fluorescence measurements in aqueous solution were carried out in a buffer comprising 50 mM Tris-HCl and 50 mM KCl (pH 8.0), with either 2.5 mM $MgCl_2$ (termed Mg^{2+}-buffer) or 1.25 mM EDTA (EDTA-buffer); solutions of N-AD(T)P in these buffers are designated by N-AD(T)P/Mg^{2+} and N-AD(T)P/EDTA, respectively. As an exception, pH-dependence of the naphthoyl fluorescence was measured in 50 mM potassium phosphate buffer. In most experiments using binary aqueous mixtures of organic solvents, the aqueous part consisted also of Mg^{2+}-buffer; however, identical results were obtained with EDTA-buffer. The percentage of organic solvent is given in v/v. Solvent mixtures with a higher amount of less polar solvent (over 50% dioxane, for example) were degassed prior to use.

All experiments were performed at 20 °C, except when indicated.

Equilibrium binding studies

Determination of equilibrium binding data (number of binding sites and dissociation constants) was based on direct titration experiments, performed by adding different amounts of enzyme to a given concentration of the respective ligand in the desired buffer; each point of a titration curve was obtained in a separate experiment, in order to take into account the limited stability of F_1 in aqueous solution. The fluorescence intensity was recorded when the signal was constant, i.e., the reaction had reached equilibrium (up to 30 min). For each line of experiments (di- or triphosphate derivative, absence or presence of Mg^{2+}) several titrations with different concentrations of the respective ligand (between 100 nM and 100 μM)

were performed. The results were combined in "indirect" binding curves ($c_{\text{ligand (bound)}}/c_{\text{enzyme}}$ vs. $c_{\text{ligand (free)}}$; see Fig. 3), from which the equilibrium binding constants were calculated by non-linear least-squares fit, under consideration of different binding models (for details, see Ref. 22).

Results

Fluorescence properties of 3′-O-(1-naphthoyl)adenosine diphosphate

Absorption spectrum and fluorescence spectra of N-ADP in aqueous medium (pH 8.0) are given in Fig. 1; the respective spectra of N-AMP and N-ATP are identical within the given precision of the measurements, implying no influence of the β- and γ-phosphate on the chromophore. (This applies to all fluorescence properties described in this chapter.) The quantum yield, Φ_F, of N-ADP in aqueous media is high, 0.58, independent of the excitation wavelength (280–320 nm). Similar fluorescence properties were found for nearly all (tested) esters of 1-naphthoic acid (for example, see the spectra of the methyl ester given in Fig. 1; $\Phi_F = 0.68$), and also for 1-naphthoic acid at low pH values, i.e., in its undissociated form; in the deprotonated form fluorescence is reduced to less than 0.5% (if not completely).

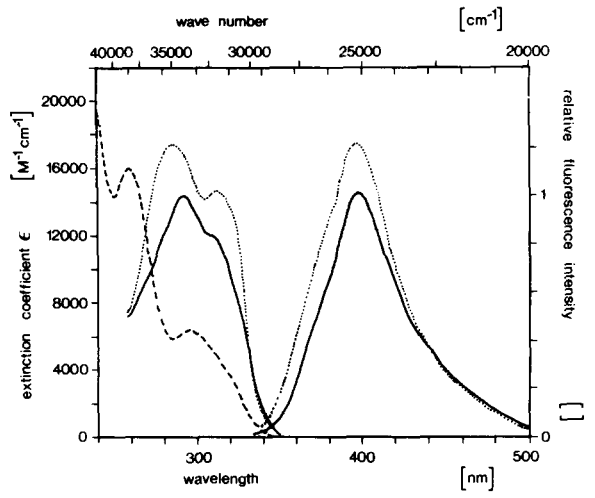

Fig. 1. Spectral properties of naphthoic acid esters. Absorption (------) and fluorescence emission and excitation spectra (———) of N-ADP, emission and excitation spectra of naphthoic acid methyl ester (· · · · · ·). All fluorescence spectra are corrected; for convenience, the spectra are given on a wavelength scale. The emission spectra are normalized by the extinction at the excitation wavelength (295 nm).

The fluorescence properties of N-ADP are independent of the proton concentration over a wide range of pH values (5.0–10.0). In more acidic media the quantum yield is higher, reaching a maximum at pH 3.0 (0.80; 0.72 at pH 4.0, 0.73 at pH 2.0); shape and wavelength position of the fluorescence spectra are unaffected. In alkaline media (pH > 10) considerable hydrolysis of the ester bond occurs, which can be monitored by the decrease of the fluorescence emission due to the negligible fluorescence of the naphthoate anion. Treated as pseudo-first-order reaction (high excess of OH^-), the rate constant was determined to be 0.24 $M^{-1} \cdot s^{-1}$ at 20 °C.

Whereas absorption spectrum (including extinction coefficient) and fluorescence excitation spectrum of the naphthoyl system are nearly insensitive to the polarity of the surrounding medium, the emission spectrum shows polarity-dependent changes (see Fig. 2). With decreasing polarity, the spectrum is blue-shifted; calculated by the average wave number, this shift amounts to 1200 cm^{-1} (or 18 nm) upon transition from water to dioxane (average wavenumber: 25200 cm^{-1} = 397 nm in water; 26400 cm^{-1} = 379 nm in dioxane). In contrast to this clearly expressed signal, other fluorescence parameters change only slightly (e.g., wavelength position of the net emission maximum) or give even ambiguous results (e.g., quantum yield).

The same polarity-dependence was found for the emission spectrum of 1-naphthoic acid methyl ester; due to its higher solubility in unpolar media, with this compound even solvents of extremely low polarity could be probed (e.g., 28800 cm^{-1} = 347 nm in *n*-pentane).

To quantitate the polarity at the binding sites for N-AD(T)P on mitochondrial F_1-ATPase, we defined a new parameter, the ratio of the emission intensity at 395 nm divided by that at 375 nm, called Q_I. The Q_I value not only describes the wavelength position of the emission spectrum, but also takes into account the polarity-dependence of the superimposed vibrational structure; thus, the resulting responses upon changes of medium polarity are pronounced ($Q_I = 1.8$ in water; 1.0 in dioxane). However, the main reason for prefering

Q_I to the average wavenumber was its relatively easy experimental accessibility, especially regarding kinetic measurements (parallel experiments with emission wavelengths of 395 and 375 nm, respectively, in contrast to the recording of emission spectra).

Because quenching normally decreases only quantum yield and related parameters, it exerts no influence on shape and wavelength position of the emission spectrum; thus, the Q_I value is not affected by adding a collisional quencher (sodium iodide) to N-ADP solutions in water or binary solvent systems. From the decrease of the fluorescence intensity upon addition of different concentrations of iodide, we calculated (Stern-Volmer equation) for aqueous media a quenching constant, k_q, of $7.1 \cdot 10^9$ $M^{-1} \cdot s^{-1}$, which is within the normal range for a freely accessible chromophore (diffusion-controlled reaction).

Due to the fluorescence lifetime of 6.3 ns, the anisotropy of free ligand is almost negligible when observed in water (viscosity about 1 mPa · s (1 centipoise); see Fig. 4B). In more viscous media, obtained by an increasing percentage of glycerol, a pronounced excitation polarization spectrum becomes visible (for example, see the reference spectrum in Fig. 4A, measured in 87% glycerol). The respective spectra show that the excitation band is made up of two electronic transitions with dipole moments oriented at an angle to each other; for technical reasons, the spectra could not be extended to wavelengths below 260 nm to give exact (presumably negative) anisotropies for the transition of higher energy. For the lower-energy transition (λ_{exc} 325 nm), from a Perrin plot of reciprocal anisotropy versus reciprocal viscosity (T/η; T was held constant) the limiting anisotropy, A_0, was calculated to be 0.29; for the rotational correlation time, a value of about 0.4 ns was determined (in water).

Equilibrium binding of 3'-O-(1-naphthoyl)adenosine phosphates to F_1-ATPase

Upon addition of F_1-ATPase, the fluorescence emission spectra of N-ADP and N-ATP change significantly. The extent of this effect is a function of the concentration of the enzyme and can be saturated, reflecting the equilibrium binding of the ligand to F_1. The emission spectrum of N-ADP at 'saturation' with enzyme is given in Fig. 2; as can be seen from the shape of the spectrum, the polarity of the environment of the naphthoyl residue has changed upon binding. However, the polarity effect alone cannot explain the resulting spectrum completely. A pronounced quench was observed by comparison with N-ADP spectra of corresponding Q_I value obtained in model experiments; in this special case, an identical Q_I was measured in a binary aqueous mixture containing 52% dioxane (see first part of Results and Table II). Although the quantum yield in enzyme-bound state is reduced to about 50% of the reference value, the fluorescence lifetime is nearly identical (6.0 ns for N-ADP bound in presence of Mg^{2+}, compared to 6.1 ns for N-ADP in 52% dioxane). This result led to the conclusion of static quenching being responsible for the diminished quantum yield, caused by formation of a complex between the ground-state of the fluorophore and the 'quencher' (an amino-acid residue at the binding domain, electronically interacting with the naphthoyl moiety of the nucleotide analogue).

In order to determine number and affinity of binding sites for N-ADP and N-ATP on F_1-ATPase by the fluorescence of the ligand, the following conditions were chosen:
To minimize inner filter effects by added protein, we used an excitation wavelength of 310 nm; this is about 12 nm above the absorption maximum, but still gives a high experimental sensitivity ($\epsilon\Phi_F$). The fluorescence emission was measured at 395 nm. Although the net emission signal is due to two independent phenomena (polarity and quenching), its registration at a single wavelength is permissible for equilibrium binding studies, as revealed by control experiments in which the integral emission spectrum was recorded after the reaction had reached equilibrium. Based on these spectra, discrimination between both effects resulted in identical standardized titration curves, with either 'polarity' or 'quenching' as ordinate.

For bound ligand, the emission intensity at 395 nm is between 30% and 50% of that of the free chromophore, the exact value depending on the absence or presence of Mg^{2+} and on the number of phosphate residues (di- or triphosphate) (see Table I). In all cases, stoichiometric titration curves reached the 'saturation' plateau in a monophasic

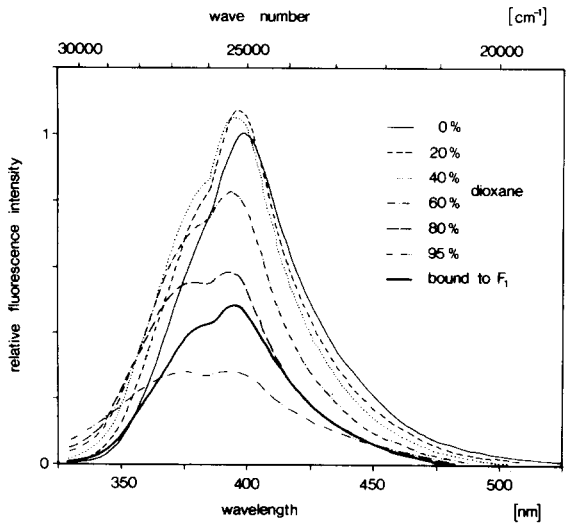

Fig. 2. Polarity dependence of N-ADP fluorescence. Thin lines give emission spectra (not corrected) in dioxane/buffer mixtures; percentage of dioxane (v/v) given in the figure, concentration of N-ADP 1 μM. The thick solid line shows the emission spectrum of N-ADP bound to F_1 (1 μM N-ADP and 2 μM enzyme in Mg^{2+}-buffer) in equilibrium.

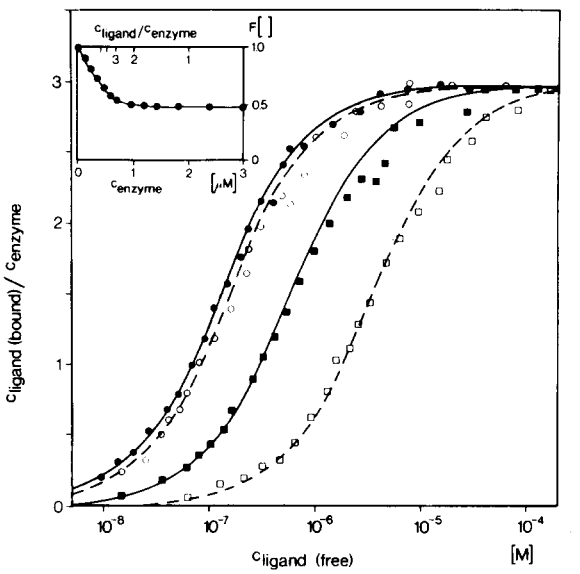

Fig. 3. Equilibrium binding of N-AD(T)P to F_1-ATPase. Data were obtained from several direct titration experiments (example given in the inset: titration of 2 μM N-ADP in Mg^{2+}-buffer with enzyme), with different concentrations of ligand (100 nM–100 μM). Experimental conditions were as follows: N-ADP/Mg^{2+} (●), N-ATP/Mg^{2+} (○), N-ADP/EDTA (■), N-ATP/EDTA (□). The curves shown were calculated on the basis of a model with three equivalent and independent binding sites; for further details, see Materials and Methods and text.

descent, resulting in a binding stoichiometry of 3 mol ligand per mol enzyme; no further change in fluorescence occurred upon decreasing the overall stoichiometry (mol ligand/mol enzyme) from this maximum to lower values (for example, see the inset in Fig. 3), thus showing the fluorescence decrease to be identical for all three subsequently bound ligand molecules.

Titrating N-AMP with F_1, the resulting quench was below 5% and did not reach saturation within the tested range of concentrations (up to 100 μM ligand and 10 μM enzyme); if present, this residual signal could be explained by inner filter effects and/or binding with extremely low affinities.

The results of the equilibrium binding experiments are given in Fig. 3 as semi-logarithmic plots. As expected from the stoichiometric titrations, saturation is reached at a value of about three molecules of N-ADP or NAP-ATP per molecule enzyme; this result is independent of the presence of Mg^{2+}, whereas the affinities are significantly lower without Mg^{2+}, especially for N-ATP. In all cases, the best fit of theoretical curves to the experimental data was obtained assuming a priori equivalent and dependent binding sites; the intrinsic dissociation constants given in Table I are based on this model. The data suggest a lower affinity of the third binding site, induced by preceding occupation of the two other sites. However, the extent of this possible negative cooperativity is quite small; the respective dissociation constants differ by factors of less than 2. In addition, it has to be taken into account that at high concentrations of (free) ligand the scatter is larger due to methodical reasons. Thus, the 'simpler' model with three equivalent and independent binding sites should also be taken into consideration; the theoretical curves given in Fig. 3 were calculated on the basis of this model, using the (identical) k_d values for the first two occupied sites.

As described in the first part of Results, the shape of the emission spectrum, represented by the Q_I value, allows a quantification of the polarity at the binding site(s). The corresponding percentage of dioxane in binary aqueous mixtures,

TABLE I

EQUILIBRIUM BINDING OF N-AD(T)P TO F_1-ATPase

ΔF, change of fluorescence intensity at saturation (λ_{exc} 310 nm, λ_{em} 395 nm); N, number of binding sites; k_{di}, intrinsic dissociation constant for the ith site; constants were calculated assuming a model with a priori equivalent and dependent sites. For details, see Materials and Methods and text.

Ligand	Condition	ΔF (%)	N	k_{d1} (nM)	k_{d2} (nM)	k_{d3} (nM)
N-ADP	Mg^{2+}	55	3.0	120	120	140
N-ADP	EDTA	70	3.0	570	550	1080
N-ATP	Mg^{2+}	57	3.1	160	160	250
N-ATP	EDTA	53	3.1	3500	3400	5800

resulting in the respective Q_I value, is listed in Table II. The values for N-ATP/Mg^{2+}, N-ATP/EDTA, and N-ADP/Mg^{2+} are rather similar, whereas for N-ADP bound in absence of Mg^{2+} the environment of the fluorophore seems to be less polar.

These results were supported by investigation of the susceptibility of bound N-AD(T)P towards quenching by iodide (data also given in Table II). Compared to free N-AD(T)P, the quenching constants, k_q, are lowered by factors between 5 and 10, showing a drastically hindered electronical interaction between iodide and the naphthoyl moiety in enzyme-bound state. In analogy to the polarity data, the k_q value for N-ADP in absence of Mg^{2+} is considerably below those for N-ATP/Mg^{2+}, N-ATP/EDTA, and N-ADP/Mg^{2+}. Again, the results are independent of the binding stoichiometry.

TABLE II

INTERACTION OF N-AD(T)P WITH THE HIGH-AFFINITY BINDING SITES OF F_1-ATPase

Lines 1–4 give the respective data for ligand bound to F_1 under the indicated experimental conditions; the listed properties are as follows. Polarity is described as corresponding percentage of dioxane; k_q, quenching constant for iodide; A, anisotropy (λ_{exc} 325 nm); E_r, relative efficiency of energy-transfer. For comparison, the respective values for free N-ADP are shown in line 5 (results for N-ATP identical). Further details given in Materials and Methods and in the next.

Ligand	Condition	Dioxane (%)	$k_q \cdot 10^{-9}$ ($M^{-1} \cdot s^{-1}$)	A	E_r
N-ADP	Mg^{2+}	52	1.2	0.27	0.81
N-ADP	EDTA	75	0.5	0.25	0.40
N-ATP	Mg^{2+}	58	1.4	0.26	0.83
N-ATP	EDTA	60	1.0	0.25	0.06
N-ADP (free)		0	7.1	0.016	0

As described in Ref. 7, the fluorescence anisotropy of N-ADP can be utilized to determine its binding to F_1-ATPase; we extended these investigations on the basis of results obtained in model experiments (see part 1). Fig. 4A gives as examples the excitation polarization spectra of N-ADP/EDTA and N-ATP/Mg^{2+} bound to the enzyme; the spectra for N-ADP/Mg^{2+} upon 'titration' with F_1 are shown in Fig. 4B. The resulting anisotropies are nearly constant for excitation wavelengths above 320 nm; for bound ligand, they amount to values between 0.25 and 0.27 (see Table II), which is below the limiting anisotropy, A_0, of 0.29. This depolarization is not only due to rotation of the naphthoyl residue relative to the protein; theoretical considerations, taking into account the fluorescence lifetime of bound N-AD(T)P (6.0 ns) and the rotational correlation time of the holoprotein, relate a part of the depolarization to some rotational motion of the enzyme (see Materials and Methods). Assuming the additional depolarization as due to fast restricted motion of the fluorescent probe over the surface of a cone, for this cone half-angles between 9° (anisotropy 0.27) and 16° (0.25) could be estimated; in these calculations, any partial rotational motion of the subunits carrying the binding domains relative to the holoenzyme is neglected.

For comparison, in Fig. 4A is also shown a spectrum of free N-AD(T)P, whose rotational motion is hindered by the viscosity of the medium. At excitation wavelengths above 320 nm, the selected reference spectrum shows an anisotropy identical with that of bound ligand; in contrast, at

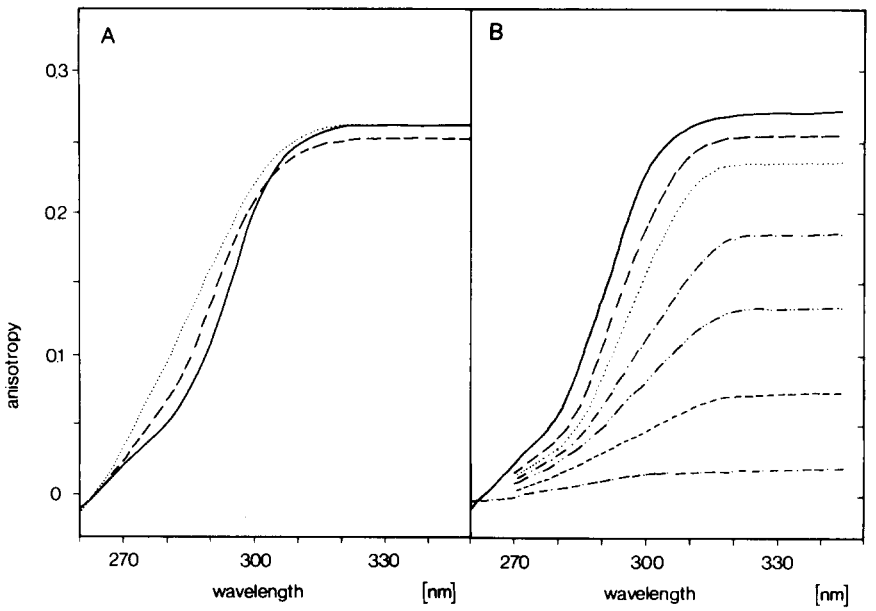

Fig. 4. Excitation polarization spectra of N-AD(T)P upon binding to to F_1. (A) Spectra of N-ATP/Mg^{2+} (———) and N-ADP/EDTA (— — —) bound to the enzyme (1.5 μM ligand, 6 μM F_1); (· · · · · ·) spectrum of free N-ADP in 87% glycerol. (B) Spectra of N-ADP (1.5 μM in Mg^{2+}-buffer), free (– – · · – –), and in presence of different concentrations of F_1: 0.12 μM (------), 0.23 μM (· · – · · – · · – · ·), 0.35 μM (· – · – ·), 0.46 μM (· · · · · ·), 0.58 μM (— — —), and 2.3 μM (———); in the last case, the ligand is completely in the enzyme-bound state.

lower wavelengths a significant depolarization can be observed for the analogue in enzyme-bound state. This indicates the contribution of a second chromophore to the total anisotropy in this case. The effect is more expressed in presence of Mg^{2+} than in its absence, reaching maximal values ($A_{glycerol/water}/A_{bound}$) at about 280 nm.

Whereas the anisotropy for $\lambda_{exc} > 320$ nm was found to be independent of the number of occupied sites, like other parameters described above ('ground-state' quenching, polarity, accessibility for iodide), this apparently does not hold for excitation wavelengths below this value. Evaluation of the titration experiment shown in Fig. 4B gave a higher degree of depolarization for high stoichiometries (ligand per enzyme).

When bound N-AD(T)P is excited by unpolarized light, the excitation spectra (Fig. 5) show a more or less pronounced additional band with a maximum at 279 nm, corresponding to the excitation spectrum of the protein [7]. In absence of ligand, no protein fluorescence emission is detectable at 395 nm, revealing this band as due to singlet-singlet energy transfer ('Förster transfer' [23]) between tyrosine residues in the protein (donor; λ_{exc} 279 nm) and N-AD(T)P (acceptor); the energy-transfer also accounts for the depolarization described above.

The relative efficiency of energy-transfer depends on the concentration of Mg^{2+}. In Fig. 5 the spectra under both 'extreme' conditions, excess of Mg^{2+} (2.5 mM) as well as excess of EDTA (1.25 mM), are given, demonstrating good agreement with the results of the respective depolarization experiments (Fig. 4). Whereas in presence of Mg^{2+} the values are similar for di- and triphosphate analogues, in presence of EDTA the efficiencies are reduced by factors of about 2 (N-ADP) and more than 10 (N-ATP), respectively (Table II). Mg^{2+} could be substituted for by Mn^{2+}, exerting the same effect; with Ca^{2+} the transfer efficiency is slightly decreased, but is still significantly higher than that in the absence of divalent cation (relative value for N-ATP 0.70; for comparison, see Table II).

In all binding experiments described above,

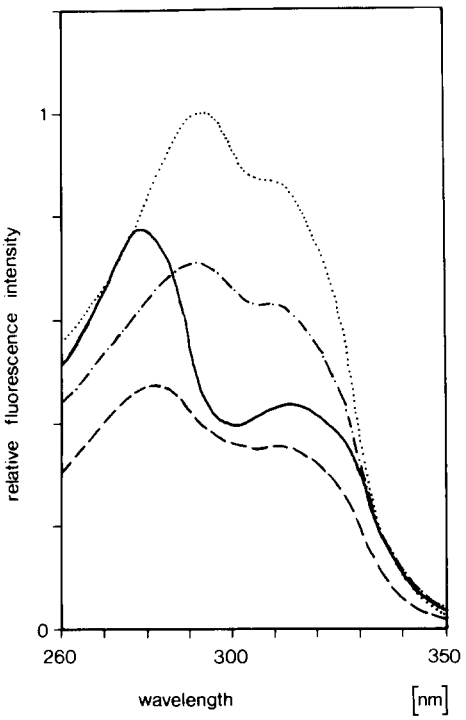

Fig. 5. Excitation spectra of N-AD(T)P bound to F_1. Spectra of 1.5 μM analogue with 1.5 μM F_1 under the following conditions: N-ADP/EDTA (------), N-ATP/EDTA (·-·-·), N-ADP/Mg^{2+} (———); the spectrum for N-ATP/Mg^{2+} does not differ significantly from the last one. For comparison, also the excitation spectrum of free N-AD(T)P (1.5 μM) is given (·····).

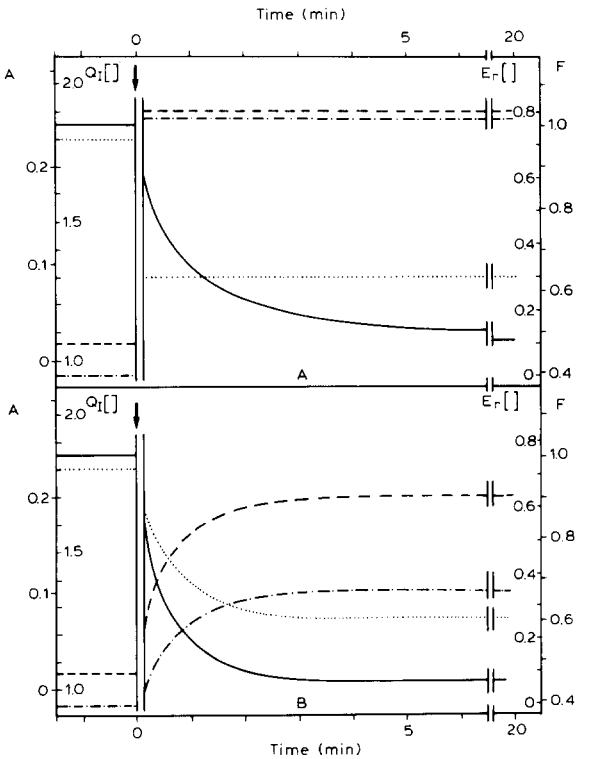

Fig. 6. Kinetics of N-ADP binding to F_1. At $t = 0$ min, indicated by the arrow, F_1 (final concentration 1.5 μM) was added to a solution of N-ADP (final concentration 1.5 μM) in Mg^{2+}-buffer (A) and in EDTA-buffer (B), respectively. The observed fluorescence parameters are designated as follows: anisotropy, A (λ_{exc} 325 nm) (— — —); Q_I (·····); relative transfer efficiency, E_t (·-·-·); relative fluorescence intensity, F (λ_{exc} 310 nm, λ_{em} 395 nm) (———).

fluorescence was measured when the signal had stabilized (between 2 and 30 min after mixing of the reactants). Investigations of the kinetics revealed the binding process as biphasic in presence of Mg^{2+}; Fig. 6A shows as an example the time-course of some parameters of N-ADP fluorescence upon binding to F_1 in Mg^{2+}-buffer. Similar results were obtained for the binding of N-ATP/Mg^{2+} to the enzyme. Polarity, described by the Q_I value, fluorescence anisotropy, and relative energy-transfer efficiency reach equilibrium immediately after mixing (less than 10 s); assuming a second-order reaction, the rate constant, k_1, was estimated to be higher than $1 \cdot 10^6\ M^{-1} \cdot s^{-1}$.

In contrast, the ground-state quenching occurs rather slowly (Fig. 6A). Variation of the ratio of concentrations of enzyme to ligand does not cause significant changes of the time-course, indicating this process as first-order. Nevertheless, attempts to describe the reaction by the rate constant or the half-time failed: The half-time, τ, is not constant during the progress of the reaction, revealing that it occurs in several subsequent steps. τ increases from initial values of about 0.5 min for N-ADP and 1 min for N-ATP, respectively, to more than 10-fold these values.

When the overall stoichiometry is raised from 1 : 1 to 2 : 1 and 3 : 1 by adding ligand (N-ADP or N-ATP) to established equilibrium complexes, this second, slow reaction phase is also observed. Analogous results are obtained when in the 1 : 1 complexes the naphthoyl derivatives are substituted for by the natural ligands ADP and ATP, respectively (all experiments carried out in presence of 2.5 mM Mg^{2+}). These findings reveal that

the slow formation of the 'ground-state quenching complex' occurs at each binding site separately and independently, and is not due to a single process upon binding of the first ligand or upon transition of the enzyme into an active state (preincubation by ATP).

This slow reaction step could not be related either to other time-dependent processes described for F_1, like progressive inhibition, observed for ATP/Mg^{2+} [24] or ADP/Mg^{2+} [25]: F_1, preincubated with N-ATP for different times (10 s–30 min), was submitted to displacement experiments with ATP as well as to ATPase activity tests; the results were found to be independent of the preincubation time. This regards time-course of displacement, final amount of bound analogue, and enzymatic activity (data not shown).

In the absence of Mg^{2+}, the time-courses of all fluorescence parameters investigated are similar (for example, see Fig. 6B); the rate constants for the 'first' reaction step, accompanied by change of polarity, anisotropy, and transfer efficiency, are drastically reduced (about $2 \cdot 10^4$ $M^{-1} \cdot s^{-1}$ for N-ATP, $4 \cdot 10^4$ $M^{-1} \cdot s^{-1}$ for N-ADP, as estimated from experiments carried out under pseudo-first-order conditions, using an excess of enzyme). On the other hand, the 'second' step (manifested by the static quenching) is accelerated. As a result, the first reaction becomes the rate-determining step, making both processes indistinguishable.

Discussion

The results presented in the first part of this study reveal the general versatility of esters of 1-naphthoic acid as fluorescent environmental probes. The particular compounds under investigation, 3′-*O*-(1-naphthoyl)adenosine phosphates, possess an additional favourable structural property: the nucleotide is modified at the ribose moiety. Since for many nucleotide-binding enzymes only base and phosphate residues are directly involved in the recognition process, this implies that the probe is not located directly at the responsible amino acid residues of the protein. Thus, influence of the present derivatization upon the binding specificity should be minimized.

Several parameters of the N-A(T)P fluorescence were used to investigate the nucleotide binding sites on mitochondrial F_1-ATPase depleted of endogenous nucleotides. The large decrease of fluorescence intensity upon binding, due to polarity effects and ground-state quenching, gives an appropriate signal to determine equilibrium binding constants. Under the conditions applied in the described experiments, it would have been possible to detect binding sites with dissociation constants up to about 200 μM. In this range, F_1 exhibits three sites for N-ADP or N-ATP. In presence of Mg^{2+}, the k_d values are far below 1 μM, confirming previous data, which had been obtained by two different fluorescence spectroscopic approaches [7]. The discrepancy in the number of detectable binding sites ($N = 2$ in Ref. 7), when measured via fluorescence anisotropy, is most likely due to depolarization by energy-transfer from tyrosine to naphthoyl residues. Since this effect is not uniform for all binding stoichiometries, experiments using excitation wavelengths within the range of protein absorption (300 nm in Ref. 7) may yield erroneous results *. In contrast, with a λ_{exc} of 325 nm also titration experiments observing the anisotropy of N-AD(T)P showed saturation at 3 mol ligand bound per mol enzyme (see also Fig. 4B).

Absence of Mg^{2+} (and other divalent cations) does not change the number of binding sites, whereas the affinity is significantly decreased. Similar behaviour has been found for the natural ligand ADP, as can be seen from comparison of the data given in Ref. 7 (with Mg^{2+}) and recently in [26] (with EDTA). However, the strong negative cooperativity, observed in both cases, is not present with N-ADP or N-ATP as ligands. As suggested in Ref. 7, these analogues are able to 'break' anticooperativity, at least partially; the results presented cannot rule out an induced slightly lower affinity for occupation of the third binding site.

However, other findings support the assumption of a model with three equivalent and independent binding sites; several fluorescence parameters, describing structural and electronical characteristics of the binding domains, were found to

* Thus, also the stoichiometry ($N = 2$) for binding of N-ATP to F_1 from the thermophilic bacterium PS3, given in a recent study [9], might be underestimated (λ_{exc} 310 nm in Ref. 9).

be independent of the binding stoichiometry, thus showing no influence of a possible cooperative interaction on these properties.

These investigations revealed for bound ligands a rather unpolar environment, a highly hindered accessibility for iodide anions (as a quencher) and a low residual mobility of the naphthoyl moiety; however, differences could be detected comparing N-ADP and N-ATP, and, especially with N-ADP, comparing the situation in presence and absence of Mg^{2+}, respectively. For the diphosphate analogue bound in absence of divalent cations, a different conformation appears probable, causing for the naphthoyl residue an even less polar environment and an even better protection against quenching. Nevertheless, in all cases the results support the binding sites to be quite deeply embedded in the protein; it should be noted that these conclusions were derived from observing a fluorophore for which at the binding domains space is not necessarily provided.

The most prominent effect of Mg^{2+} (and some other divalent cations) upon the properties of the binding sites is its influence on energy transfer from tyrosine residues in the protein to the naphthoyl substituent of the nucleotide. Assuming a value of 2/3 for the orientation factor, κ^2, the characteristic transfer distance, R_0, for the donor-acceptor pair tyrosine/naphthoyl adenosine phosphate was calculated to be 2.1 nm; however, in the special case of F_1/N-AD(T)P no statement can be made about the justification of this assumption. In addition, in view of 98 tyrosine residues present in F_1 [15], with possible energy-transfer between themselves, and with different distances from or orientations towards the ligand(s), a quantitative attribution of transfer efficiencies or the assignement of a specific tyrosine residue at the binding domain as the 'donor' appears impossible. In fact, the 'donor' may consist of an assembly of several tyrosine side-chains with more-or-less efficient transfer of excitation energy towards the probe molecules.

Nevertheless, occurrence of a conformational rearrangement at the binding domain upon addition of Mg^{2+} is obvious. In these conformational changes tyrosine residues are involved. On the basis of the present results, it is not possible to differenciate whether the enhanced transfer efficiency in presence of Mg^{2+} is due to variation in R (reduced distance between donor and acceptor) or in R_0, i.e., κ^2, caused by different orientation of the transition dipole moments of donor and acceptor; probably, both values, R as well as κ^2, are subject to change. Under consideration of the reservations made above, the results of the energy-transfer experiments might be taken as a further support for the essential role of tyrosine side-chains at the nucleotide binding site(s) [27–29].

An important observation is the occurrence of a biphasic nucleotide binding process in presence of Mg^{2+}, which is obviously identical at all three binding sites. The analogues, N-ADP as well as N-ATP, are bound to the sites with a high rate constant (over $1 \cdot 10^6$ $M^{-1} \cdot s^{-1}$), resembling that found for the natural ligand ATP ($6.4 \cdot 10^6$ $M^{-1} \cdot s^{-1}$ [30]). In this initially formed enzyme-ligand complex, the naphthoyl residue is already exposed to a rather unpolar environment and has a restricted rotational mobility. The second phase consists of a slow conformational rearrangement causing static quenching, probably in several subsequent steps, as indicated by the non-uniform half-time. The range of this rearrangement appears to be rather limited: even the spatial relationship between the naphthoyl residue and the tyrosine moieties acting as donor of the energy-transfer is not influenced. Unimolecular conformational changes have been described for many enzyme-ligand complexes [31]; however, in this special case the reaction is apparently extraordinarily slow ($\tau > 30$ s, compared to about 1 to $1 \cdot 10^{-4}$ s [31]), at least with the analogues under investigation. A similar biphasic process has been suggested for the binding of *lin*-benzo-ADP to F_1 (in presence of Mg^{2+}) [2]. However, this conclusion was only based on the finding of biphasic quenching; direct experimental support for the first phase being the 'binding' step was lacking. In contrast, this could be proved in this study for the binding of N-AD(T)P/Mg^{2+}.

Interestingly, absence of Mg^{2+} does not only cause the (expected) decreased rate constants of the binding phase, but also appears to accelerate the conformational rearrangement. This influence of divalent cations on the kinetics of the binding process and on the conformation of the binding

domains, as well as a recently observed effect of inorganic phosphate, will be investigated in more detail in further experiments.

Acknowledgements

The authors would like to thank A. Flauss and D. Mutschall for skillful technical assistance, J. Kasper for preparation of the drawings, and Dr. H. Tiedge for stimulating discussions.

References

1 Tondre, C., and Hammes, G.G. (1973) Biochim. Biophys. Acta 314, 245–249
2 Kauffman, R.F., Lardy, H.A., Barrio, J.R., Barrio, M.C.G., and Leonard, N.J. (1978) Biochemistry 17, 3686–3692
3 Matsuoka, I., Watanabe, T., and Tonomura, Y. (1981) J. Biochem. 90, 967–989
4 Grubmeyer, C., and Penefsky, H.S. (1981) J. Biol. Chem. 256, 3718–3727
5 Tiedge, H., and Schäfer, G. (1986) Biol. Chem. Hoppe-Seyler 367, 689–694
6 Vignais, P.V., and Lunardi, J. (1985) Annu. Rev. Biochem. 54, 977–1014
7 Tiedge, H., Lücken, U., Weber, J., and Schäfer, G. (1982) Eur. J. Biochem. 127, 291–299
8 Schäfer, G., and Weber, J. (1982) J. Bioenerg. Biomembranes 14, 470–498
9 Rögner, M., Gräber, P., Lücken, U., Tiedge, H., Weber, J., and Schäfer, G. (1986) Biochim. Biophys. Acta 849, 121–130
10 Onur, G., Schäfer, G., and Strotmann, H. (1983) Z. Naturforsch. 38c, 49–59
11 Schäfer, G., Lücken, U., and Lübben, M. (1986) Methods Enzymol. 126, 682–712
12 Weast, R.C., (ed.) (1985) CRC Handbook of Chemistry and Physics, p. C-365, CRC Press, Boca Raton
13 Penin, F., Godinot, C., and Gautheron, D. (1979) Biochim. Biophys. Acta 548, 63–71
14 Lowry, O.H., Rosebrough, N.J., Farr, A.L. and Randall, R.J. (1951) J. Biol. Chem. 193, 265–275
15 Walker, J.E., Fearnley, I.M., Gay, N.J., Gibson, B.W., Northrop, F.D., Powell, S.J. Runswick, M.J., Saraste, M., and Tybulewicz, V.L.J. (1985) J. Mol. Biol. 184, 677–701
16 Vogel, G., and Steinhart, R. (1976) Biochemistry 15, 208–216
17 White, C.E., and Argauer, R.J. (1970) Fluorescence Analysis: A Practical Approach, pp. 30–53, Marcel Dekker, New York
18 Scott, T.G., Spencer, R.D., Leonard, N.J., and Weber, G. (1970) J. Am. Chem. Soc. 92, 687–695
19 Jameson, D.M., Weber, G., Spencer, R.D., and Mitchell, G. (1978) Rev. Sci. Instrum. 49, 510–514
20 Tiedge, H., Schäfer, G., and Mayer, F. (1983) Eur. J. Biochem. 132, 37–45
21 Dale, R.E., and Eisinger, J. (1975) in Biochemical Fluorescence Concepts (Chen, R.F., and Edelhoch, H., eds.), Vol. 1, pp. 115–284, Marcel Dekker, New York
22 Peters, F., and Lücken, U. (1986) Methods Enzymol. 126, 733–740
23 Förster, T. (1948) Ann. Physik 2, 55–75
24 Lowe, P.N., and Beechey, R.B. (1981) Biochem. J. 196, 433–442
25 Di Pietro, A., Penin, F., Godinot, C., and Gautheron, D. (1980) Biochemistry 19, 5671–5678
26 Lunardi, J., Klein, G., and Vignais, P.V. (1986) J. Biol. Chem. 261, 5350–5354
27 Hollemans, M., Runswick, M.J., Fearnley, I.M., and Walker, J.E. (1983) J. Biol. Chem. 258, 9307–9313
28 Garin, J., Boulay, F., Issartel, J.P., Lunardi, J., and Vignais, P.V. (1986) Biochemistry 25, 4431–4437
29 Bullough, D.A., and Allison, W.S. (1986) J. Biol. Chem. 261, 14171–14177
30 Grubmeyer, C., Cross, R.L., and Penefsky, H.S. (1982) J. Biol. Chem. 257, 12092–12100
31 Hammes, G.G., and Schimmel, P.R. (1970) in The Enzymes (Boyer, P.D., ed.), Vol. 2, pp. 67–114, Academic Press, New York